

# Synthesis of metal oxide nanorods using carbon nanotubes as templates

B. C. Satishkumar,<sup>a</sup> A. Govindaraj,<sup>a,b</sup> Manashi Nath<sup>a</sup> and C. N. R. Rao<sup>\*a,b</sup>

<sup>a</sup>Chemistry and Physics of Materials Unit and CSIR Centre of Excellence in Chemistry, Jawaharlal Nehru Centre for Advanced Scientific Research, Jakkur P. O., Bangalore 560 064, India. E-mail: cnrrao@jncaasr.ac.in

<sup>b</sup>Solid State and Structural Chemistry Unit, Indian Institute of Science, Bangalore 560 012, India

Received 10th April 2000, Accepted 14th June 2000

Published on the web 19th July 2000

Nanorods of several oxides, with diameters in the range of 10–200 nm and lengths upto a few microns, have been prepared by templating against carbon nanotubes. The oxides include V<sub>2</sub>O<sub>5</sub>, WO<sub>3</sub>, MoO<sub>3</sub> and Sb<sub>2</sub>O<sub>5</sub> as well as metallic MoO<sub>2</sub>, RuO<sub>2</sub> and IrO<sub>2</sub>. The nanorods tend to be single-crystalline structures. Nanotube structures have also been obtained in MoO<sub>3</sub> and RuO<sub>2</sub>.

## 1. Introduction

The preparation of metal oxide nanocomposites and oxide fibres by using carbon nanotubes as removable templates was first reported by Ajayan *et al.*,<sup>1</sup> who prepared such materials based on V<sub>2</sub>O<sub>5</sub>. Carbon nanotubes have been converted to nanorods of metal carbides by reaction with volatile oxide or halide species.<sup>2</sup> The reaction of gallium oxide vapor with carbon nanotubes in the presence of ammonia gives rise to GaN nanorods,<sup>3</sup> while the reaction of silicon oxide vapor in a nitrogen atmosphere gives silicon nitride nanorods.<sup>4</sup> Metal oxide nanotubes have been prepared by using carbon nanotubes as templates, with particular success in the case of zirconia.<sup>5,6</sup> Metal oxide nanostructures have been prepared by the use of sol-gel chemistry within the pores of alumina and polymer membranes.<sup>7</sup> We have found that carbon nanotubes can be effectively used as templates to obtain nanostructures of metal oxides. We have prepared nanorods of V<sub>2</sub>O<sub>5</sub>, WO<sub>3</sub>, MoO<sub>3</sub>, Sb<sub>2</sub>O<sub>5</sub>, MoO<sub>2</sub>, RuO<sub>2</sub> and IrO<sub>2</sub> in good yields, the last three being metallic. Furthermore, most of the nanorods are single-crystalline structures. Nanotube structures of the oxides have also been obtained in some instances.

## 2. Experimental

The method of preparation of metal oxide nanorods and nanotubes makes use of multi-walled carbon nanotubes (MWNTs). The MWNTs were prepared by the arc vaporization of graphite rods in a helium atmosphere (550 Torr) at 30 V, 100 A direct current.<sup>8</sup> The nanotubes formed in the core region of the cathode deposit were dispersed in methanol and sonicated for 2 hours in a separating funnel. The bulky graphitic carbon was removed from the suspension. The remaining solid suspension was allowed to settle, dried and heated in air at 700 °C for 20 minutes to oxidize the graphitic carbon.<sup>9</sup> The pure carbon nanotubes thus obtained were closed at either end or open at one end in some instances. They were treated with boiling HNO<sub>3</sub> for 24 h. Such nanotubes are almost always open and contain a considerable number of acidic sites on the surface.<sup>10,11</sup> The concentration of surface acidic sites is around  $6 \times 10^{20}$  sites g<sup>-1</sup> of nanotubes. The acid-treated nanotubes were washed with water and dried in an oven at 60 °C for 12 h. The nanotubes so obtained had an inner diameter in the range of 2–8 nm and an outer diameter in the

range of 10–30 nm (length up to 1 μm). The acid-treated carbon nanotubes were coated with an appropriate oxide precursor such as an alkoxide and dried at 100 °C, followed by calcination at 450 °C. The calcined sample was heated at 700 °C in air to burn off the carbon. While generally we got nanorods by this method, in some instances we got nanotubes as well.

The experimental procedure for preparing the oxide nanostructures is as follows: In order to prepare V<sub>2</sub>O<sub>5</sub> coated carbon nanotubes, aqueous sodium meta-vanadate was first passed through a cation exchange column (DOWAX) to get vanadic acid (HVO<sub>3</sub>). 100 mg of acid-treated carbon nanotubes were stirred with 2 ml of HVO<sub>3</sub> for 48 h. The excess gel was removed by washing with water and acetone. The nanotubes so obtained were dried in an oven at 100 °C for 6 h.

In the case of WO<sub>3</sub> and MoO<sub>3</sub>, an aqueous solution of Na<sub>2</sub>WO<sub>4</sub> or Na<sub>2</sub>MoO<sub>4</sub> was passed through a cation exchange column. The resulting tungstic or molybdic acid (H<sub>2</sub>WO<sub>4</sub> or H<sub>2</sub>MoO<sub>4</sub>) was used for coating the acid-treated carbon nanotubes (100 mg) by magnetic stirring for 48 h. The excess tungstic or molybdic acid was washed off with water. The nanotube sample was dried at 100 °C for 6 h. To coat the nanotubes with Sb<sub>2</sub>O<sub>5</sub>, the acid-treated nanotubes (100 mg) were mixed with 2 ml of SbCl<sub>5</sub> and stirred for 48 h. The sample was filtered and washed with methanol and dried at 100 °C for 6 h.

In the case of RuO<sub>2</sub>, the gel was obtained by the reaction of aqueous RuCl<sub>3</sub> (Aldrich) with NaOH. The gel was washed repeatedly with distilled water to remove free Na<sup>+</sup> and Cl<sup>-</sup> ions. 100 mg of the acid-treated carbon nanotubes were stirred with the gel for 48 h. The sample was dried at 100 °C for 6 h and treated with H<sub>2</sub>O<sub>2</sub> to oxidize Ru<sup>3+</sup> to Ru<sup>4+</sup>. The resulting nanotubes were dried at 100 °C for 6 h and calcined at 450 °C for 12 h.

Anhydrous IrCl<sub>3</sub> (Aldrich) was fused with NaOH to obtain Na<sub>2</sub>IrCl<sub>6</sub>. This was diluted with distilled water to get an intensely blue-colored solution. 100 mg of acid-treated carbon nanotubes were stirred with this solution for 48 h. The sample was washed with distilled water and dried at 100 °C for 6 h.

After the oxide-coated nanotubes were heated in air at 700 °C (except in the case of V<sub>2</sub>O<sub>5</sub> where it was 500 °C), the oxide nanostructures obtained were subjected to X-ray diffraction (XRD), scanning electron microscopy (SEM) and transmission electron microscopy (TEM).

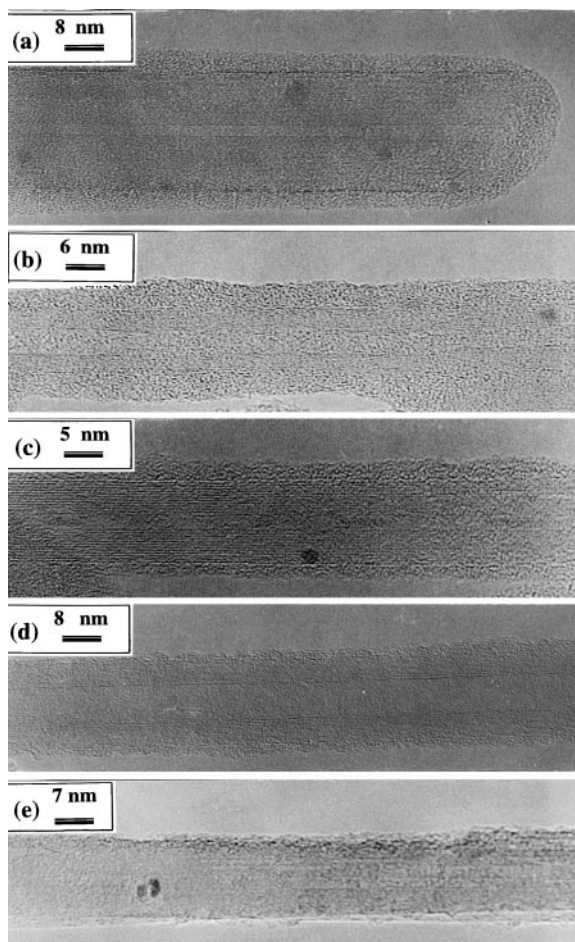


**Fig. 1** HREM images of carbon nanotubes coated with (a)  $V_2O_5$ , (b)  $WO_3$ , (c)  $MoO_3$ , (d)  $RuO_2$  and (e)  $IrO_2$  obtained on calcination of the oxide-coated carbon nanotubes at  $450^\circ C$  for 12 h.

### 3. Results and discussion

The calcined samples of different oxide-coated carbon nanotubes revealed the presence of satisfactory coverage of the oxidic material as shown in the typical TEM images in Fig. 1. Thus, the high resolution electron microscopic (HREM) image of the nanotubes coated with  $V_2O_5$  in Fig. 1(a) shows that the oxidic coating is uniform throughout the length of the nanotube. The situation is similar with the other oxide coatings as can be seen from the images in Fig. 1(b)–(e). The strong interaction of the oxidic material with the surface of the carbon nanotube is due to the presence of surface acidic sites, resulting from the acid treatment.<sup>10,11</sup>

On the removal of the nanotube template, the resulting oxidic species showed the presence of interesting nanostructures. In Fig. 2(a) we show the SEM image of  $V_2O_5$  obtained after the removal of the template. The image shows the presence of copious quantities of nanorods. A TEM bright-field image of the  $V_2O_5$  nanorods is shown in Fig. 2(b). The nanorods have diameters in the range of 20–55 nm and are 2–3  $\mu m$  long. The selected area electron diffraction (SAED) pattern on a nanorod shows the presence of regular spots due to (110) and (200) planes as shown in the inset of Fig. 2(b), signifying the single crystalline nature of the  $V_2O_5$  nanorods. The zone axis projection is along  $[10\bar{2}]$  of the orthorhombic  $V_2O_5$ . The XRD pattern of the oxide powder showed it to be orthorhombic, with unit cell parameters of  $a=11.44 \text{ \AA}$ ,  $b=3.54 \text{ \AA}$  and  $c=4.35 \text{ \AA}$ , in agreement with the literature values (JCPDS file: 9-387). The template could be removed at a relatively lower temperature in the case of  $V_2O_5$ , since it catalyzes the oxidation of the carbon nanotubes.

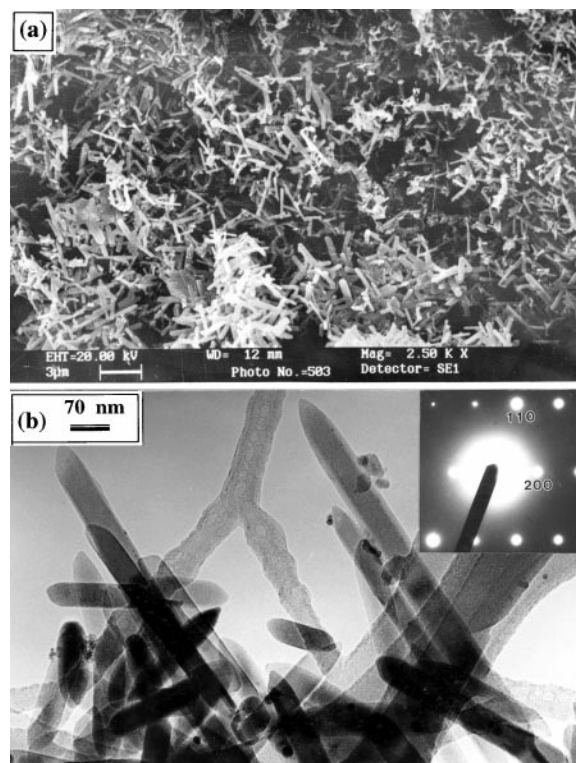


**Fig. 2** (a) SEM image of  $V_2O_5$  nanorods and (b) TEM image of a  $V_2O_5$  nanorod. The inset shows the SAED pattern taken on a nanorod.

In the case of  $WO_3$ , SEM observations indicated a relatively low yield of the nanorods. A typical TEM image of the  $WO_3$  nanorods is shown in Fig. 3(a). The diameter of the nanorods is in between 15 and 60 nm. The TEM image in Fig. 3(b) shows a relatively long nanorod, with a length of 5  $\mu m$ . The SAED pattern shown in the inset of Fig. 3(b) indicates a zone axis projection along  $[010]$ , with the Bragg spots corresponding to the (001) and (200) planes of monoclinic  $WO_3$ . The XRD pattern of the oxide powder gave unit cell parameters of the monoclinic phase ( $a=7.331 \text{ \AA}$ ,  $b=7.52 \text{ \AA}$  and  $c=7.71 \text{ \AA}$  with  $\beta=90.1^\circ$ , JCPDS file: 24-747).

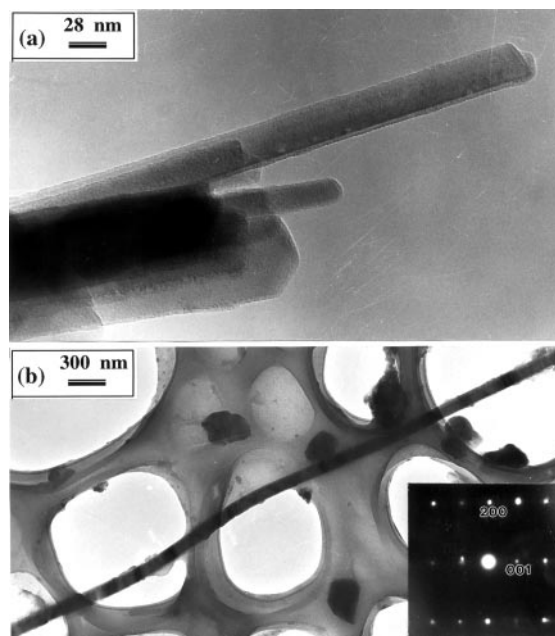


**Fig. 3** (a) TEM image of nanorods of  $WO_3$  after removal of carbon template at  $700^\circ C/12 \text{ h}$ . (b) TEM image of a relatively long nanorod. Inset shows the SAED pattern of a nanorod showing a zone axis projection along  $[010]$ .

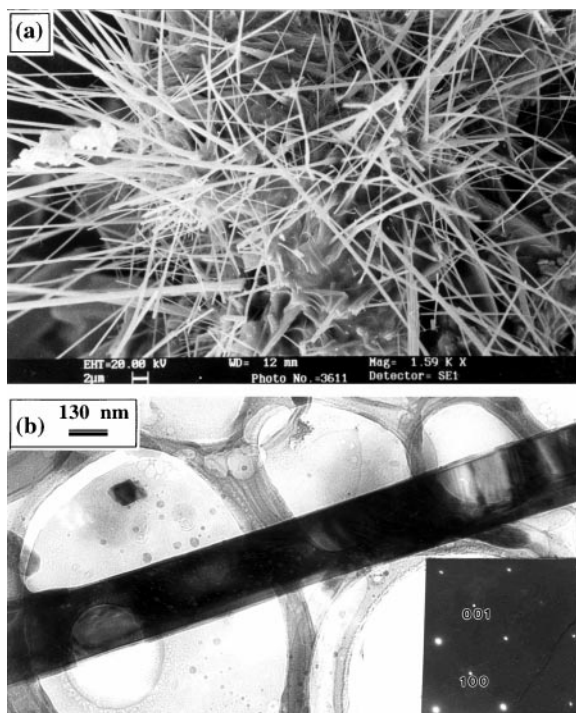


**Fig. 4** (a) SEM image of MoO<sub>3</sub> nanorods and (b) TEM image of a nanorod. The inset in (b) shows the SAED pattern along the [010] direction.

We obtained nanorods of MoO<sub>3</sub> in high yields (after template removal at 600 °C for 12 h), as revealed by the SEM image in Fig. 4(a). The diameter of the nanorods is in the 80–150 nm range, with the length in the 5–15 μm range. By subjecting the MoO<sub>3</sub>-coated carbon nanotubes to repeated washing (before calcination), we were able to obtain thinner nanorods of the oxide, after removal of the template. The TEM image of a MoO<sub>3</sub> nanorod is shown in Fig. 4(b). The SAED pattern revealing the single crystalline nature of the nanorod is shown in the inset of Fig. 4(b). The XRD pattern gave the orthorhombic unit cell parameters,  $a = 3.96 \text{ \AA}$ ,  $b = 13.85 \text{ \AA}$  and  $c = 3.7 \text{ \AA}$  (JCPDS file: 35-609).

Sb<sub>2</sub>O<sub>5</sub> gave short nanorods in relatively good yields. The

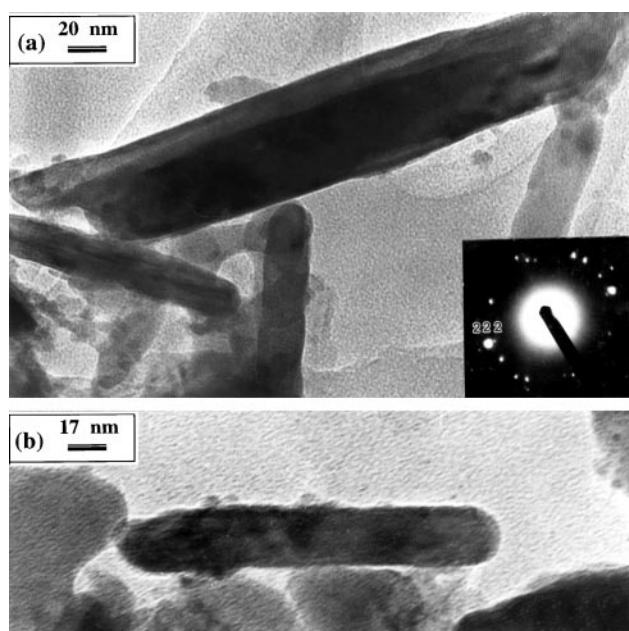


**Fig. 5** (a) and (b) TEM images of Sb<sub>2</sub>O<sub>5</sub> nanorods obtained on removal of the template at 600 °C/12 h. The SAED pattern of the nanorods is shown in the inset of (a).

TEM image of the nanorods is shown in Fig. 5(a). The image in Fig. 5(b) shows the TEM image of an isolated nanorod of Sb<sub>2</sub>O<sub>5</sub>. The nanorods have diameters in the range of 10–60 nm and lengths in the range 100–400 nm. The SAED pattern shown as an inset in Fig. 5(a) reveals bright spots due to the (222) planes. The XRD pattern showed it to have a cubic structure with the cell parameter,  $a = 10.98 \text{ \AA}$  (JCPDS file: 5-534).

While the nanostructures discussed above are all of nonmetallic oxides, we sought to prepare nanorods of metallic oxides such as MoO<sub>2</sub>, RuO<sub>2</sub> and IrO<sub>2</sub>. In order to obtain MoO<sub>2</sub> nanorods, nanorods of MoO<sub>3</sub> were reacted with hydrogen at 500 °C for 48 h. The SEM and TEM images of MoO<sub>2</sub> nanorods are shown in Fig. 6(a) and (b) respectively. The nanorods are 150–300 nm in diameter and 5–10 μm long. The SAED pattern of the nanorod (see inset of Fig. 6(b)) shows the projection along the [010] direction. The XRD pattern showed the presence of a monoclinic phase with the unit cell parameters,  $a = 5.60 \text{ \AA}$ ,  $b = 4.85 \text{ \AA}$  and  $c = 5.54 \text{ \AA}$  with  $\beta = 119.4^\circ$  (JCPDS file: 32-671).

A TEM image of the RuO<sub>2</sub> nanorods is shown in Fig. 7(a). The nanorods are single-crystalline in nature as indicated by the SAED pattern given as an inset in Fig. 7(a). It shows the projection along the [001] direction. The nanorods have diameters in the 5–20 nm range and are 50–200 nm long. An HREM image of a RuO<sub>2</sub> nanorod is shown in Fig. 7(b). The image shows the lattice planes with  $d = 3.1 \text{ \AA}$  corresponding to (110) planes of tetragonal RuO<sub>2</sub>. The XRD pattern confirmed the tetragonal structure with the tetragonal unit cell parameters,  $a = 4.48 \text{ \AA}$  and  $c = 3.12 \text{ \AA}$  (JCPDS file: 40-1290).

IrO<sub>2</sub> also gave a relatively good yield of nanorods. In this case, we also observed an intermediate oxide structure, after heat-treating the oxide-coated carbon nanotubes at 500 °C. This temperature is slightly lower than that required for the complete removal of the carbon template. We show a TEM image of this structure in Fig. 8(a). HREM observations showed the polycrystalline nature for the intermediate nanostructure. It appears that during the template removal,

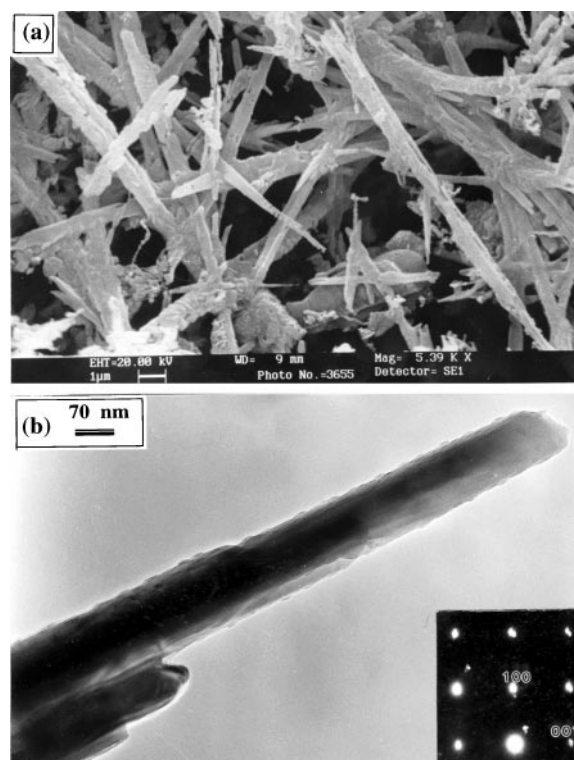


**Fig. 6** (a) SEM image and (b) TEM image of nanorods of MoO<sub>2</sub> obtained by the treatment of MoO<sub>3</sub> nanorods with H<sub>2</sub> at 500 °C for 48 h. Inset in (b) shows the zone axis projection along [010].

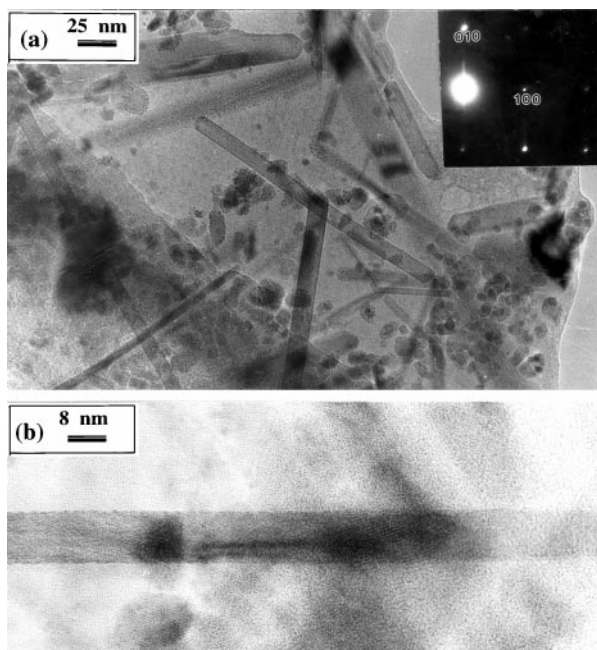


**Fig. 7** (a) TEM image of RuO<sub>2</sub> nanorods and (b) HREM image of a RuO<sub>2</sub> nanorod showing the (110) planes. The inset in (a) shows the SAED pattern of a nanorod. The small particles seen in the image are also due to the oxide.

the oxide coatings on neighboring carbon nanotubes coalesce to form the rod-like nanostructures. Up to a certain temperature the nanorod formed is polycrystalline, and becomes single-crystalline around 600 °C. This is seen from the TEM image of the IrO<sub>2</sub> nanorods in Fig. 8(b). The diameter of the nanorods is in the range of 30–60 nm and the length goes up to 1 μm. The

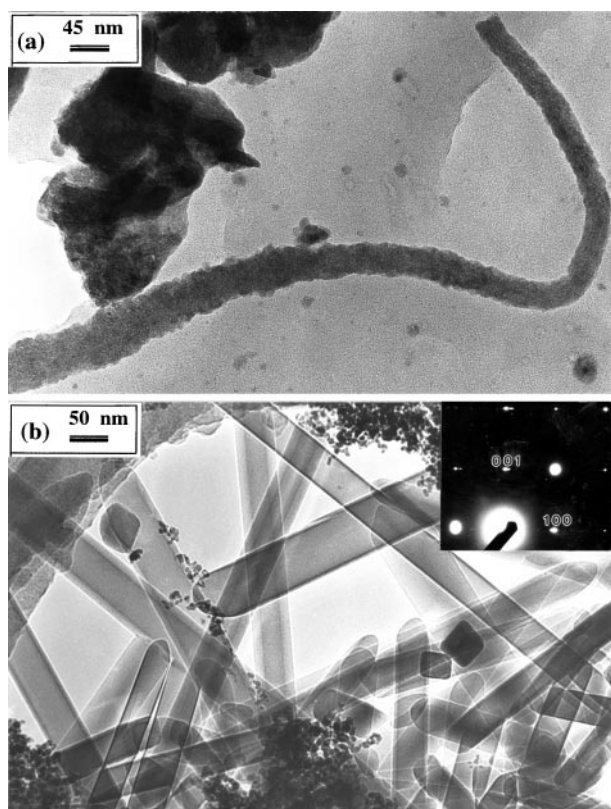


**Fig. 8** TEM images of (a) intermediate nanostructure of IrO<sub>2</sub> obtained on heat-treatment of oxide-coated carbon nanotubes at 500 °C for 12 h and (b) nanorods of IrO<sub>2</sub> obtained after the complete removal of carbon template at 600 °C for 12 h. The SAED pattern of a nanorod is shown as the inset.

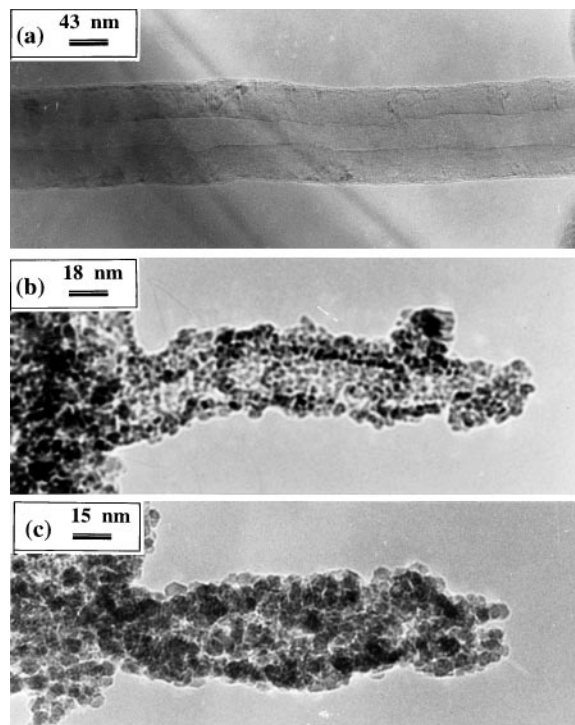


**Fig. 9** (a) TEM image of a MoO<sub>3</sub> nanotube and (b), (c) TEM images of nanotube-like structures of RuO<sub>2</sub>.

inset in Fig. 8(b) shows the SAED pattern of a single nanorod, with the spots arising from the (100) and (001) planes of tetragonal IrO<sub>2</sub>. The XRD pattern revealed the rutile phase with the unit cell parameters,  $a = 4.50 \text{ \AA}$  and  $c = 3.15 \text{ \AA}$  (JCPDS file: 15-870). It is noteworthy that both RuO<sub>2</sub> and IrO<sub>2</sub> are metallic.

The formation of single-crystalline nanorods in the present study is noteworthy. A possible mechanism of formation of such nanorods may be as follows. CO or/and CO<sub>2</sub> is produced when the oxide-coated carbon nanotubes are heated, the oxygen being (at least partly) derived from the coated oxide. Subsequently, the remaining metal or sub-oxide may get reoxidized and undergoes recrystallization. Another possibility is that the decomposition of the oxide precursor in the hot combustion zone of the nanotubes gives rise to the crystals *in situ*. The crystals could get elongated because of the evolution of gases during the transformation. The precursor decomposition also gives H<sub>2</sub>O or/and CO<sub>2</sub>.

In some of the preparations, we obtained nanotube structures of the oxide, in addition to the nanorod structures. In Fig. 9(a) we show the TEM image of a MoO<sub>3</sub> nanotube. The inner diameter of the oxidic nanotube is 23 nm. Nanotube-like structures of RuO<sub>2</sub> are also obtained in some preparations. TEM images of such structures are shown in Fig. 9(b) and (c). The nanotube in RuO<sub>2</sub> is not as well formed and we barely see a nanotube shape in the TEM images. The nanotube comprises the stable rutile phase.

#### 4. Conclusions

In conclusion, the present study establishes that nanorods of a variety of metal oxides can be readily prepared by using carbon nanotubes as templates. The method also offers certain advantages. Thus, most of the preparations yield single-crystalline nanorods of fairly large dimensions. Furthermore, the nanorods are generally much longer than the starting nanotube template. The observation of oxide nanotubes in some cases is also significant.

## References

- 1 P. M. Ajayan, O. Stephan, Ph. Redlich and C. Colliex, *Nature*, 1995, **375**, 564.
- 2 H. Dai, E. W. Wong, Y. Z. Lu, S. Fan and C. M. Lieber, *Nature*, 1995, **375**, 769.
- 3 W. Han, S. Fan, Q. Li and Y. Hu, *Science*, 1997, **277**, 1287.
- 4 W. Han, S. Fan, Q. Li, B. Gu, X. Zhang and D. Yu, *Appl. Phys. Lett.*, 1997, **71**, 2271.
- 5 B. C. Satishkumar, A. Govindaraj, E. M. Vogl, L. Basumallick and C. N. R. Rao, *J. Mater. Res.*, 1997, **12**, 604.
- 6 C. N. R. Rao, B. C. Satishkumar and A. Govindaraj, *Chem. Commun.*, 1997, 1581.
- 7 B. B. Lakshmi, C. J. Patrissi and C. R. Martin, *Chem. Mater.*, 1997, **9**, 2544.
- 8 C. N. R. Rao, R. Seshadri, A. Govindaraj and R. Sen, *Mater. Sci. Eng.*, 1995, **R15**, 209.
- 9 R. Seshadri, A. Govindaraj, H. N. Aiyer, R. Sen, G. N. Subbanna, A. R. Raju and C. N. R. Rao, *Curr. Sci. (India)*, 1994, **66**, 839.
- 10 R. M. Lago, S. C. Tsang, K. L. Lu, Y. K. Chen and M. L. H. Green, *J. Chem. Soc., Chem. Commun.*, 1995, 1355.
- 11 B. C. Satishkumar, A. Govindaraj, J. Mofokeng, G. N. Subbanna and C. N. R. Rao, *J. Phys. B, Atm. Mol. Opt. Phys.*, 1996, **29**, 4925.